

Severe Feto-Placental Abnormalities Precede the Onset of Hypertension and Proteinuria in a Mouse Model of Preeclampsia¹

Anuja Dokras,^{3,4} Darren S. Hoffmann,^{3,5} Joshua S. Eastvold,⁵ Martha F. Kienzle,⁵ Lynn M. Gruman,⁵ Patricia A. Kirby,⁶ Robert M. Weiss,^{7,8} and Robin L. Davisson^{2,5,8}

Departments of Obstetrics and Gynecology,⁴ Anatomy and Cell Biology⁵ Pathology,⁶ Internal Medicine and Veterans Affairs,⁷ and The Cardiovascular Center,⁸ Roy J. and Lucille A. Carver College of Medicine, The University of Iowa, Iowa City, Iowa 52242

ABSTRACT

Preeclampsia is a prevalent and potentially devastating disorder of pregnancy. Characterized by a sudden spike in blood pressure and urinary protein levels, it is associated with significant obstetric complications. BPH/5 is an inbred mouse model of preeclampsia with borderline hypertension before pregnancy. BPH/5 mice develop hypertension, proteinuria, and endothelial dysfunction during late gestation (after E14.5). We hypothesized that BPH/5 mice might exhibit early feto-placental abnormalities before the onset of maternal disease. All placental cell lineages were present in BPH/5 mice. However, the fetal and placental weights were reduced, with abnormalities in all the placental zones observed starting early in gestation (E9.5–E12.5). The fractional area occupied by the junctional zone was significantly reduced at all gestational timepoints. Markedly fewer CDKN1C-stained trophoblasts were seen invading the proximal decidual zone, and this was accompanied by reductions in *Cdkn1c* gene expression. Trophoblast giant cell morphology and cytokeratin staining were not altered, although the mRNA levels of several giant cell-specific markers were significantly downregulated. The labyrinth layer displayed decreased branching morphogenesis of endothelial cells, with electron microscopy evidence of attenuated trophoblast layers. The maternal decidual arteries showed increased wall-to-lumen ratios with persistence of actin-positive smooth muscle cells. These changes translated into dramatically increased vascular resistance in the uterine arteries, as measured by pulse-wave Doppler. Collectively, these results support the hypothesis that defects at the maternal-fetal interface are primary causal events in preeclampsia, and further suggest the BPH/5 model is important for investigations of the underlying pathogenic mechanisms in preeclampsia.

decidua, gene regulation, placenta, pregnancy, trophoblast

INTRODUCTION

Preeclampsia is a pregnancy-specific disorder defined by the sudden onset of hypertension and proteinuria in the second half

of pregnancy (>20 weeks). Relatively common and with a 40% increase in the incidence of preeclampsia over the last fifteen years [1], this multi-system syndrome is associated with substantial risks for both mother and baby. It is the leading cause of maternal death and a major contributor to perinatal morbidity and mortality worldwide [2, 3]. Despite its common occurrence and serious consequences, treatment of preeclampsia has not changed over the last 150 years. Even today, the only known effective means to avoid catastrophic progression to overt eclampsia is early delivery of the fetus.

Despite considerable research efforts, the cause of this devastating disorder remains elusive. Two obstacles have hindered progress in understanding the pathogenesis of preeclampsia. First, in the clinical setting, research has mostly been limited to observations and interventions in mid-to-late pregnancy when maternal symptoms manifest, which is probably long after the disease-causing events are set in motion. Second, the lack of relevant animal models of preeclampsia has hampered basic research into disease mechanisms.

Recently, our group has reported the first non-primate animal model that spontaneously develops the clinical sequelae of preeclampsia. The inbred mouse strain BPH/5 exhibits frank hypertension and proteinuria starting in the last trimester of pregnancy (days 14–21). These symptoms, as in humans, resolve upon delivery [4]. Late gestation in BPH/5 mothers is further characterized by endothelial dysfunction and renal glomerulosclerosis, which are additional hallmarks of the disease in women [4]. In the non-pregnant state, BPH/5 females are normal with regard to each of these parameters, with the exception of a slight elevation in basal blood pressure [4]. This latter finding prompted us to evaluate this strain for preeclampsia susceptibility, since it is known that elevated blood pressure before pregnancy or a family history of hypertension is a major risk factor for the disease [5, 6]. Importantly, this preeclampsia phenotype in BPH/5 female mice is not observed with pregnancy in other genetic animal models of hypertension. Furthermore, while there are several animal models in which aspects of preeclampsia have been induced by experimental interventions [7–10], and *Cdkn1c* knockout results in placental and maternal changes consistent with preeclampsia [11], the BPH/5 mouse strain is the first model in which the full maternal syndrome develops without any intervention. Moreover, as in human preeclampsia, the BPH/5 mice exhibit a compromised perinatal status, which includes fetal growth restriction, progressive intrauterine fetal demise, and small litters of low-birth-weight pups [4].

In addition to the maternal systemic disorder, human preeclampsia is also strongly associated with abnormal placentation. In fact, most current theories point to the placenta as a primary causative factor. Delivery, which also removes the placenta, results in resolution of the maternal symptoms

¹Supported by the American Heart Association (0540114N to R.L.D.), a predoctoral fellowship from the American Heart Association (0510021Z to D.S.H.), and a dissertation fellowship from the Woodrow Wilson National Fellowship Foundation/Johnson & Johnson (to D.S.H.).

²Correspondence: Robin L. Davisson, Department of Biomedical Sciences, T9-014C Veterinary Research Tower, Cornell University, Ithaca, NY 14853-6401. FAX: 607 253 3378; e-mail: robin.davisson@cornell.edu

³These authors contributed equally to this work.

Received: 5 May 2006.

First decision: 26 May 2006.

Accepted: 27 August 2006.

© 2006 by the Society for the Study of Reproduction, Inc.

ISSN: 0006-3363. <http://www.biolreprod.org>

associated with preeclampsia. In addition, preeclampsia can develop in pregnancies without a fetus, i.e., hydatidiform moles [12, 13], further underscoring the potential pathogenic role of the placenta.

The most striking feature of placental dysfunction in preeclampsia is the impairment of maternal decidual spiral artery remodeling that is secondary to abnormal fetal trophoblast invasion, which interferes with the timely expansion of the placental vasculature and results in insufficient uteroplacental circulation [14–16]. Normally, in the human hemochorial placenta during the first half of gestation, cytotrophoblasts differentiate into invasive extravillous cells that migrate into the endometrium, the inner-third of the myometrium, and towards the spiral arteries. Replacement of the laminar smooth muscle of the maternal spiral arteries by the invading cytotrophoblasts results in marked dilation and increased blood supply to the expanding placenta [14]. In term placental biopsies taken from preeclamptic patients, there is evidence of incomplete invasion of trophoblasts into the uterus and its vasculature [14, 17], abnormalities in cytotrophoblast differentiation that involve a change from an epithelial to endothelial phenotype [18, 19], excessive proliferation of immature intermediate trophoblasts [20], and reduced expression of genes that encode angiogenic factors and their receptors [10, 21]. Although the primary trigger for these abnormalities is unknown, it is postulated that the resulting poor placentation and reduced blood supply in early pregnancy leads to the release of factor(s) in the maternal circulation that ultimately produce the clinical features of preeclampsia [22]. Compromised placental perfusion also probably contributes to fetal growth restriction and the low birth-weights observed in pregnancies complicated by preeclampsia [23, 24].

As it is impossible to study prospectively the placentation process in humans, with most data derived from placental bed biopsies at delivery, it has proven difficult to investigate the causal links between dysregulation in early placental development and preeclampsia. The use of an animal model that consistently and spontaneously recapitulates the syndrome offers new opportunities for determining the early progression of events leading up to the clinical syndrome. As such, the goal of this study was to track longitudinally the fetoplacental phenotype of BPH/5 mice over the course of pregnancy starting early in gestation, with an eye toward further establishing this as a unique model for studying the molecular underpinnings of preeclampsia. Since human and mouse placentas are hemochorial, share many similar anatomical, cellular, and genetic features, and the layers appear to be functionally analogous [25–27], studies of placentation in the BPH/5 mice are likely to yield new insights into the pathogenesis of preeclampsia in women.

MATERIALS AND METHODS

Animals and Husbandry

Experiments were performed in female BPH/5 (in-house colony) and C57BL/6 (C57 [Harlan, Indianapolis, IN]) mice (19–24g, 8–16 wk old). As described in detail previously, BPH/5 is an inbred subline derived from the spontaneously hypertensive strain BPH/2, and C57 mice serve as a control for both strains [4, 28–31]. Timed matings were performed by pairing strain-matched males and females overnight, as described previously [4], with the morning of detection of a vaginal plug being designated as embryonic day 0.5 (E0.5). All the cohorts of animals were comprised of both primiparous and multiparous animals. Care of the mice was conducted in accordance with the standards set forth in the Guide for the Care and Use of Laboratory Animals of the National Institutes of Health. The University Animal Care and Use Committee at the University of Iowa approved all the procedures.

Histology, Immunohistochemistry, and Electron Microscopy

BPH/5 and C57 mice were killed by CO₂ asphyxiation at various gestational timepoints (E9.5–19.5). At the earlier timepoints (up to E12.5), the entire uterine horn was removed, sectioned between implantation sites and immersed en bloc in 10% neutral buffered formalin for fixation. At later gestational stages, the placenta was isolated from the fetus (uterine wall retained intact), fixed, and then embedded in paraffin wax according to standard protocols. Special care was taken to place all the placentas in a similar orientation prior to embedding. A subset of the placentas and fetuses at various gestational times were weighed prior to tissue fixation and staining.

Tissues were sectioned (4- μ m thickness) and stained with hematoxylin and eosin (H&E) for general morphology and/or subjected to immunohistochemistry using the following reagents: biotinylated Griffonia simplicifolia isolectin B4 (dilution 1:125; Vector Laboratories, Burlingame, CA), to label the basement membranes of fetal endothelial cells in the labyrinth zone [32]; anti-pancytokeratin (dilution 1:150; Sigma), to label the trophoblast cells; anti-smooth muscle actin (M0851, dilution 1:50; Dako, Carpinteria, CA), as a marker for vascular smooth muscle cells in the decidual vessels; and anti-CDKN1C (cyclin-dependent kinase inhibitor 1C, also known as p57^{Kip2}) Ab-3 (dilution 1:100; Lab Vision, Fremont, CA), to stain the glycogen-positive trophoblast cells that invade the maternal decidua [33]. Periodic acid Schiff (PAS) reagent was used to stain the granules in the uterine natural killer (uNK) lymphocytes in the decidua and the glycogen-positive cells and fibrin deposits in the spongiotrophoblast and labyrinth layers [34, 35]. The Masson Trichrome stain was used to identify the decidual arteries and measure the luminal width.

Immunohistochemical staining was performed on a Dako Autostainer (Dako), as per the manufacturer's instructions. Briefly, after antigen retrieval and blocking, slides were incubated with isolectin B4 for 2 h or anti-CDKN1C antibody for 30 min, followed by rinsing in TBST and incubation with RTU Vectastain ABC peroxidase-conjugated streptavidin reagent (Vector Laboratories) for 20 min or mouse-on-mouse biotinylated anti-mouse IgG reagent for 20 min, followed by Streptavidin Vectastain Elite ABC peroxidase-conjugated reagent. For both antibodies, the slides were stained with DAB+ (Dako) for 5 min and counterstained with H&E. PAS and Masson Trichrome staining were performed using standard protocols.

For transmission electron microscopy (TEM), semi-thin (1- μ m thickness) placental sections were collected and fixed in Karnovsky fixative for 24 h, followed by post-fixation in 1% OsO₄ with 1.5% potassium ferrocyanide and staining.

Morphometric Analysis

Morphometric analyses of placentas were performed essentially as described [36], with the aid of the NIH image analysis systems (Scion Image and Image J). All measurements were made on multiple sections taken from a plane in the center of the placenta and perpendicular to its flat (fetal) side. Samples were stained as described above to identify the major zones, which in the murine placenta include the fetal labyrinth, junctional zone (containing spongiotrophoblasts, glycogen-containing trophoblasts, and trophoblast giant cells) and maternal decidua [36–38]. The width of the placenta was determined by drawing a line parallel to the base of the labyrinth, identifying the midpoint of this line, and then extending a perpendicular line first to the outer edge of the junctional zone (identified by morphological detection of trophoblast giant cells) and then up to the peripheral edge of the decidua (Fig. 1, A and B). The space occupied by the placenta was expressed as the ratio of the relative width of the labyrinth plus junctional zones (placenta, P) and decidua (De) (P:P+De). To determine the cross-sectional area occupied by the junctional zone (JZ), the labyrinth (L) was first measured by tracing the region that was positively stained with isolectin B4. Then, the entire area between the base of the placenta (chorioallantois, CA) and the giant cell layer (identified morphologically) was traced and measured. From this, we derived the area of the junctional zone alone and expressed it as a ratio of the total area occupied by the non-decidual areas of the placenta (JZ:JZ+L).

Morphometric analyses were also used to quantify the lumen sizes of the decidual arteries (in the central region of the decidua, from the giant cell border up to approximately 150 μ m distal) identified by Trichrome staining of placental sections (plane of sectioning same as described above). The outer diameter (OD) and luminal diameter (LD) of each vessel were measured at the point of the largest OD (Fig. 3B). The ratio of LD:OD was used to compare the proportionate luminal widths of the decidual vessels in the two strains. All measurements were made independently by two investigators who were blind to the groups, and the mean values for the two scores were used for statistical analysis.

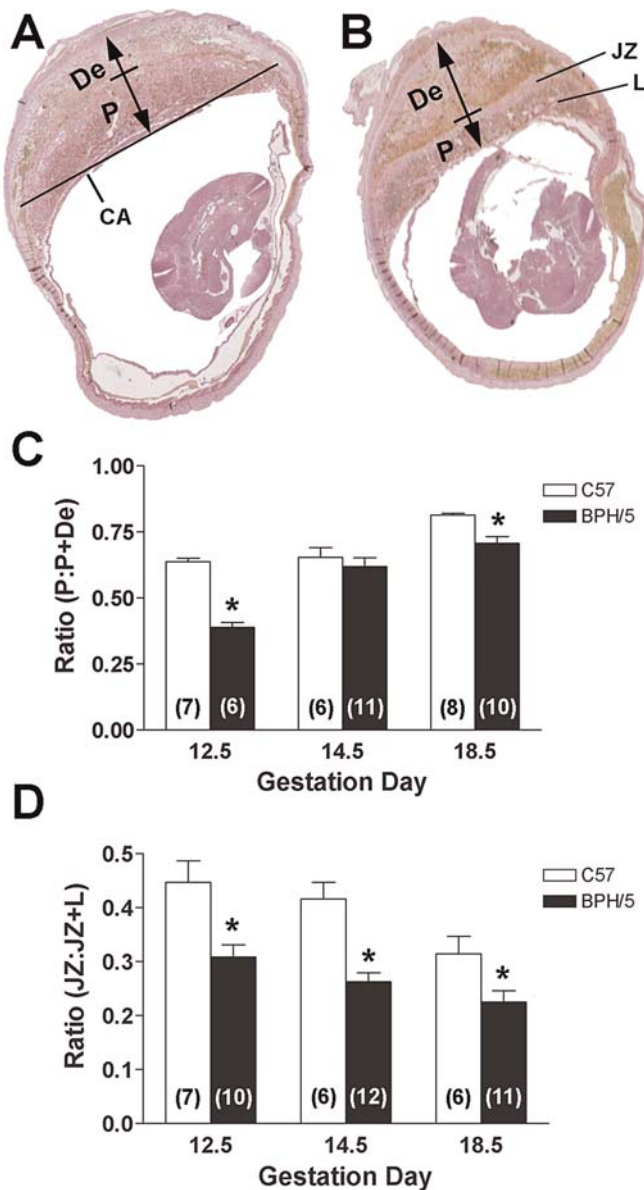


FIG. 1. The depth of the placental disc and the fractional area occupied by the junctional zone are reduced in BPH/5 mice. Representative photomicrographs of intact fetoplacental units at E12.5 from C57 (A) and BPH/5 (B) mice. Placental layers (L, labyrinth; JZ, junctional zone; De, decidua) are identified by staining with isolectin B4. The proportional depth of the placental disc (P) and the fractional area of the JZ were measured as indicated by the arrows and described in the text, with the results summarized in C and D, respectively. Data are expressed as mean \pm SEM, and the numbers of fetoplacental units measured are shown on each summary bar. * $P < 0.05$ versus C57. CA, chorioallantois.

Quantitative Real-Time RT-PCR

BPH/5 and C57 mice were killed and the placentas were collected for RNA isolation. For E9.5 conceptuses, all of the extraembryonic tissues were dissected and pooled, as described previously [39]; for the E14.5 and E19.5 timepoints, whole placentas, including the decidua but not the uterine myometrium, were collected [39]. Multiple placentas from each litter were pooled, homogenized in Trizol reagent (Molecular Research Center, Cincinnati, OH), and purified in an RNeasy spin column (Qiagen, Chatsworth, CA). DNase-treated total RNA (DNA-free; Ambion, Austin, TX) was quantified, reverse-transcribed, and the cDNA was amplified with an ABI 7000 or 7700 real-time PCR thermocycler using SYBR green (PE Biosystems, Foster City, CA) according to the manufacturers instructions. Primers designed using the Primer Express software (Applied Biosystems, Foster City, CA) are listed in Table 1 (synthesized by Integrated DNA Technologies, Coralville, IA).

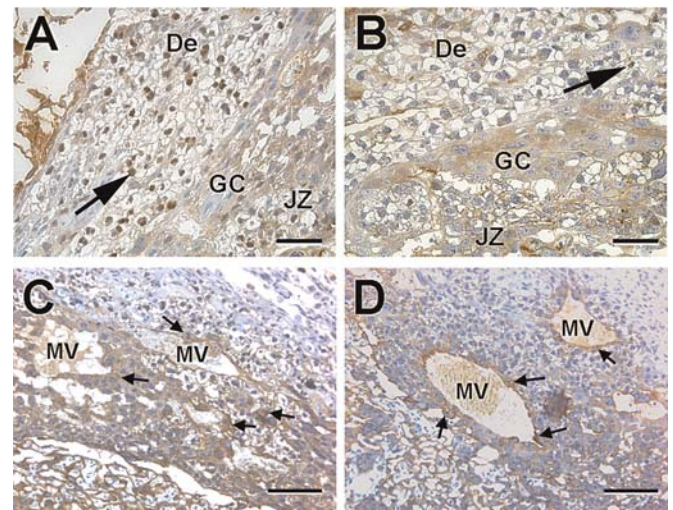


FIG. 2. Abnormalities in markers of decidual invasion. Representative image of CDKN1C-stained vacuolated trophoblast cells (arrow) invading beyond the giant cell (GC) layer into the maternal decidua (De) in C57 mice (A) at E14.5. In contrast, CDKN1C-positive cells (see arrow) are rarely seen invading into the decidua of BPH/5 placentas at this gestational age (B). This difference in CDKN1C staining between the two strains persists through E18.5 ($n = 6-11$ placentas for each strain at E14.5 and E18.5). Diffuse interstitial invasion surrounding maternal vessels (MV) in the decidua, as indicated by cytokeratin-positive trophoblasts in the central decidua, does not appear to be different between C57 (C) and BPH/5 (D) mice; $n = 6-11$ placentas for each strain at E12.5, E14.5, and E18.5. Bars = 50 μm (A and B) and 100 μm (C and D).

Experiments were run in triplicate and the gene expression levels were determined according to the standard curve method described previously (User Bulletin #2; Applied Biosystems). The transcript levels were normalized to the 18S RNA levels, and the data are expressed as fold-change relative to the C57 controls. Sequence-specific amplification was confirmed by gel analysis of the PCR products and single-peak formation during the dissociation protocol following amplification.

Ultrasound Assessment of Maternal-Placental Blood Flow

Pulse-wave Doppler was performed on BPH/5 ($n = 6$) and C57 ($n = 7$) mice at E16.5 using an Acuson Sequoia c256 imager fitted with a 15-MHz linear array oscillator/receiver, as described previously [4]. The mice were administered midazolam (0.3 mg) subcutaneously, then held gently by the nape of the neck and cradled in the hand of the sonographer. As described previously, this method produces no perturbation of the adult murine heart rate or blood pressure, no known teratogenic effects, and eliminates the need for stressful physical restraint of the animal during imaging [4, 40]. Uterine arteries were identified by the meridian color-flow along the external uterine wall. Pulse-wave depth gates were placed in the region of uterine artery color-flow, and the waveforms were analyzed offline using electronic calipers. The pulsatility index (PI) was derived from the waveforms ($\text{PI} = \text{systolic/diastolic flow velocity}$) in line with the standard clinical approach, providing an indicator of vascular resistance downstream of the artery from which the Doppler profile is acquired [41]. The PI data were converted to Resistance Index ($\text{RI} = 1 - [1/\text{PI}]$) for the analysis because of the near-cessation of diastolic flow in several of the BPH/5 mice (leading to PI values close to infinity).

Statistical Analysis

Data are expressed as mean \pm SEM. Statistical significance was determined using the Student *t*-test and differences were considered significant at $P < 0.05$.

RESULTS

Diminished Fetal Weights and Placental Masses in BPH/5 Mice

We have previously described smaller live-born litters and reduced neonatal weights for BPH/5 mice compared to C57

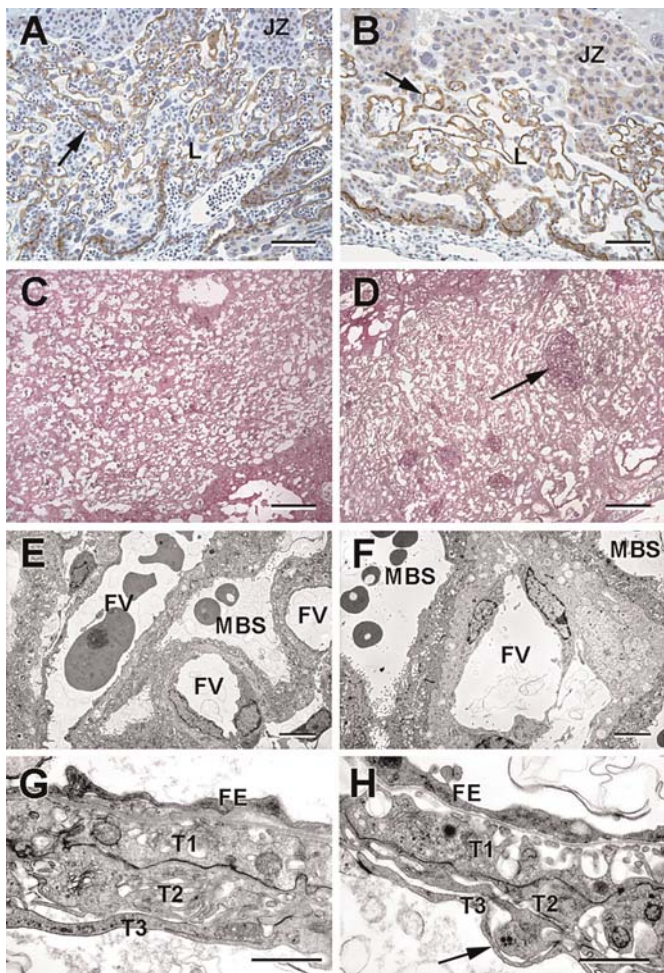


FIG. 3. Anatomical defects in the fetal labyrinth of BPH/5 placentas. **A**) Typical examples of isolectin B4-stained fetal endothelial basement membranes of C57 placentas (E12.5), showing extensive branching and elongated vessels (arrow) in the labyrinthine layer. **B**) Reduced branching morphogenesis of the fetal vessels and diminished expansion of the labyrinth towards the junctional zone (JZ) are seen in the BPH/5 placentas at E12.5. **C**) In C57 mice, PAS staining of the labyrinth zone shows a uniform distribution of trophoblasts across the feto-maternal blood spaces at E14.5. **D**) In contrast, persistence of PAS-positive trophoblast islands (arrow) is observed in BPH/5 placentas at E14.5. **E**) Representative transmission electron micrographs showing maternal blood spaces (MBS) and fetal vessels (FV) in the labyrinths of C57 placentas at E14.5. **F**) Fewer blood spaces per field are seen in BPH/5 mice compared to C57 mice at this time-point. **G**) Higher magnification imaging reveals the ultrastructure of the intervening layers between the feto-maternal blood spaces, which are composed of fetal capillary endothelium, its associated basement membrane, and a trilaminar trophoblast layer (T1–3), as shown at E19.5 in C57 placentas. **H**) In BPH/5 placentas, the three trophoblast layers are disorganized. The T1 layer shows elongated processes arising from its surface, T2 is markedly attenuated and both the T1 and T2 layers have several short projections giving these layers a porous appearance. N = 6–8 placentas for each strain. Bars = 100 μ m (**A** and **B**), 200 μ m (**C** and **D**), 10 μ m (**E** and **F**), and 1 μ m (**G** and **H**).

control mice [4]. In the present study, we report 40–50% reductions in the placental masses of BPH/5 mice at early (E9.5) and mid-gestation (E14.5) compared to those of C57 mice (Table 2). By late gestation, there were few viable fetoplacental units due to progressive demise [4]. However, of those that remained, the placental weights were similar to those of C57 mice at this gestational stage (E19.5, Table 2). Throughout pregnancy, the BPH/5 fetuses were significantly smaller than their C57 counterparts (Table 3).

Abnormalities in All Placental Zones of BPH/5 Mice Starting Early in Gestation

To evaluate further which of the placental zones contribute to the dramatic reductions in placental mass in BPH/5 mice and to provide detailed comparative analyses of placentation in this strain compared to C57, a combination of histological, immunohistochemical, morphometric, and electron microscopy studies were performed. While all the placental cell lineages were present in both strains of mice, abnormalities were detected in each of the placental zones of the BPH/5 mouse.

Depth of the placental disc. As shown in the representative photomicrographs of intact fetoplacental units (E12.5) from C57 mice (Fig. 1A) and BPH/5 mice (Fig. 1B), the proportional depth of the placental disc (P, labyrinth plus junctional zone) relative to the decidua (De) in BPH/5 mice was markedly diminished compared to that in C57 mice. The data from both groups of animals at the various timepoints are summarized in Figure 1C, and these results reveal a significant reduction in the amount of space occupied by the placenta compared to the decidua in BPH/5 mice beginning at E12.5 and through E18.5. This suggests that BPH/5 mice exhibit restricted expansion of the placenta toward the decidua starting early in gestation, and that this is maintained throughout pregnancy.

Fractional area of the junctional zone. Further morphometric analyses revealed that the reduction in placental depth in BPH/5 mice was largely due to a decrease in the fractional area occupied by the junctional zone in these mice. As summarized in Figure 1D, there was a striking reduction in the proportional area of this region at all gestational ages in BPH/5 mice compared to the C57 controls. Histological examination of the junctional layer revealed the presence of PAS-positive vacuolated cells (glycogen cells), non-vacuolated eosinophilic cells (spongiotrophoblasts), and trophoblast giant cells in both BPH/5 and C57 mice, which indicates that total loss of a specific cell type does not contribute to the observed reduction in the size.

Markers of decidual invasion. To evaluate whether there are abnormalities in the invasive properties of cells within the junctional zones of BPH/5 mice, immunohistochemical markers were used. Two types of invasion by trophoblast cells into the proximal decidua have been described for the mouse [37, 42]. Interstitial invasion refers to the subset of vacuolated glycogen-positive cells that exhibits diffuse invasion into the decidua and stains positively for the cell proliferation marker

TABLE 1. Primers used for real-time RT-PCR analysis of placental gene expression.

Target gene	Forward primer	Reverse primer
<i>Csh1</i> (chorionic somato-mammotropin hormone 1)	5'-AGAAATGCAGCTGACTTTGAATCTT-3'	5'-GGCTTGACACCAGCAGCA-3'
<i>Csh2</i> (chorionic somato-mammotropin hormone 2)	5'-TGGACCTATGGCCTGATGTTAA-3'	5'-TTGCTCGCTGTTTTCTGGAGT-3'
<i>Plf</i> (proliferin)	5'-GGCTCACACACTATTCAGCTCTTC-3'	5'-CGTCCAGAGGGCTTTCCC-3'
<i>Plfr</i> (proliferin-related protein)	5'-TGAAGCATCTCCCCGAA-3'	5'-GTTGGATCAAAGAAGGGAGCAT-3'
<i>Cdkn1c</i> (cyclin-dependent kinase inhibitor 1C [p57 ^{Kip2}])	5'-CAGCGGACGATGGAAGAACT-3'	5'-CTCCGGTTCCTGCTACATGAA-3'

TABLE 2. Placental mass (mg) in C57 and BPH/5 mice at different gestational stages.

Gestation Day	C57 ^a	BPH/5 ^a
E9.5	14.7 ± 0.22 (17)	5.8 ± 0.14 (12) ^b
E14.5	117.5 ± 1.70 (20)	65.8 ± 6.40 (25) ^b
E19.5	109.2 ± 1.50 (13)	115.6 ± 4.30 (22)

^a Data are expressed as mean ± SEM. The numbers in parentheses are the numbers of placentas in each group.

^b $P < 0.05$ versus C57.

CDKN1C [33, 42], whereas central invasion refers to the presence of cytokeratin-positive cells just beyond the giant cell layer in the center of the implantation site and usually found in a perivascular location [42]. We examined the patterns of CDKN1C and cytokeratin staining in BPH/5 and C57 placentas at early, mid-, and late-gestation. The earliest evidence of CDKN1C nuclear staining in the junctional zone of C57 placentas was at E14.5. The CDKN1C-positive cells were plentiful and had diffused beyond the giant cell layer into the maternal decidua of these mice (Fig. 2A). In contrast, at the same gestational timepoint in BPH/5 placentas, only occasional CDKN1C-positive cells were detected in the junctional zone, and few if any had diffused into the decidua (Fig. 2B). This difference in CDKN1C staining between the two strains persisted through E18.5 (data not shown). Cytokeratin-positive trophoblast cells were seen to invade the central portions of the decidua just beyond the giant cell layer and lining near the blood spaces in the proximal decidual region from E10.5 onwards in both C57 and BPH/5 placentas, although no significant differences in the abundance or localization of these cells were observed between the two strains at any timepoint (Fig. 2, C and D). In addition, artery-associated giant cells were detected in the central decidua in both strains, with no apparent difference in frequency (data not shown).

Anatomical features of the labyrinth. The labyrinth zone consists of cells of trophoblast and mesodermal origin that together undergo branching morphogenesis, resulting in a large surface area for nutrient and gas exchange between the mother and fetus. Using isolectin B4 to identify the fetal endothelial cell basement membranes [32], we compared the anatomical features of this placental zone in BPH/5 and C57 mice. At E12.5 in C57 mice, the labyrinth had uniformly elongated fetal vessels with elaborate branching morphogenesis (Fig. 3A). In contrast, the fetal vasculature of the BPH/5 placenta at this timepoint showed dramatically attenuated and irregular branching, and the extent of expansion of the labyrinth towards the junctional zone was reduced (Fig. 3B). PAS staining revealed that with increasing gestational age, the fetal vessels in the C57 placentas advanced uniformly towards the trophoblasts, such that the maternal and fetal blood spaces were separated by only a few trophoblast cells (Fig. 3C). In contrast, in the labyrinths of BPH/5 placentas, PAS-positive broad trabecular columns were seen between the fetal vessels in early gestation, and smaller clusters of trophoblast cells persisted through middle and late gestation (Fig. 3D). It is noteworthy that PAS-positive fibrin-type fibrinoid deposits that lacked trophoblasts or cellular components were also prominent in the fetal labyrinthine blood spaces in the BPH/5 placentas as early as E12.5. These fibrinoid deposits were rarely seen in C57 placentas (data not shown).

Electron microscopy was used to visualize the three trophoblast layers and fetal capillary endothelium that comprise the fetomaternal interface in the labyrinth. As shown in the electron micrographs (Fig. 3, E and F), fewer fetal and maternal blood spaces per field were observed in the BPH/5 labyrinths

TABLE 3. Fetal weights (mg) in C57 and BPH/5 mice at different gestational stages.

Gestation Day	C57 ^a	BPH/5 ^a
E12.5	87.9 ± 2.7 (17)	65.2 ± 6.2 (23) ^b
E14.5	277.3 ± 5.8 (21)	191.2 ± 6.3 (26) ^b
E18.5	1210.8 ± 14.7 (60)	1048.9 ± 54.2 (31) ^b

^a Data are expressed as mean ± SEM. The numbers in parentheses are the numbers of fetuses in each group.

^b $P < 0.05$ versus C57.

compared to the C57 labyrinths at E14.5. In addition, whereas all three trophoblast layers were easily identified and uniform in appearance in the C57 placentas, the BPH/5 placentas were characterized by attenuated and irregular trophoblast layers (Fig. 3, G and H). For example, in C57 mice, the two trophoblast layers closest to the fetal basement membrane (T1 and T2) were of similar thickness with focal junctional areas between them, and the outermost layer (T3) was more loosely attached and in contact with the maternal blood space (Fig. 3G). This is in sharp contrast to the anomalous organization of these layers in BPH/5 mice (Fig. 3H), in which the middle layer (T2) was noticeably diminished compared to T1, and both T1 and T2 exhibited a marked porous appearance. In addition, protruding elongated processes that arose from the outermost trophoblast layer were often noted. Thinning of the intervacular trophoblast layers and elongation of the outer layer may represent compensatory adaptations to increase the surface area for exchange, as described in models of fetoplacental hypoxia [43]. It should be noted that the fetal endothelium and its basement membrane were not thickened and appeared to be continuous in both the BPH/5 and C57 placentas.

Maternal decidual vessels. The main spiral arteries that supply blood to the placental bed undergo significant morphological changes as they traverse the decidua, including an increase in diameter and a concomitant decrease in smooth muscle cells. This process has been described in detail in mice (E10.5 to E14.5) and has been shown to be linked to trophoblast endo/perivascular invasion [42]. In this study, we found marked differences in this process in BPH/5 decidua. Trichrome staining revealed that whereas the C57 placentas had dilated, thin-walled arteries in the central, proximal region of the decidua at E10.5 (Fig. 4A), the vessels in this region of the BPH/5 placentas had narrowed lumens and a cuffed or onion-skin appearance, indicative of a thickened arterial wall (Fig. 4B). These differences persisted through mid-gestation (Fig. 4, C and D) and are summarized as the ratios of inner lumen-to-outer diameter ratios in Figure 4E.

In addition to a lack of vessel remodeling, the BPH/5 placentas exhibited abnormal persistence of actin-positive cells in the central vessels of the decidua at these same gestational stages (Fig. 4, F and G). After this period, actin-positive cells were rarely seen in the arterial walls in the decidua of either strain. Areas of linear necrosis accompanied by extravasations and PAS-positive fibrin-type fibrinoid deposits were also observed within the decidual layers of BPH/5 mice (Fig. 4H). These types of fibrinoid deposits were rarely seen in C57 placentas.

Granulated uNK lymphocytes are abundant in mouse decidua, especially from E12–14, and may facilitate dilation of the spiral arteries [35]. Using PAS staining, we examined the distributions of these cells in the decidua of BPH/5 and C57 placentas. PAS-positive granulated cells were widely distributed throughout the decidua in C57 and BPH/5 mice, with similar abundances and patterns between E10.5–14.5 in both strains (data not shown).

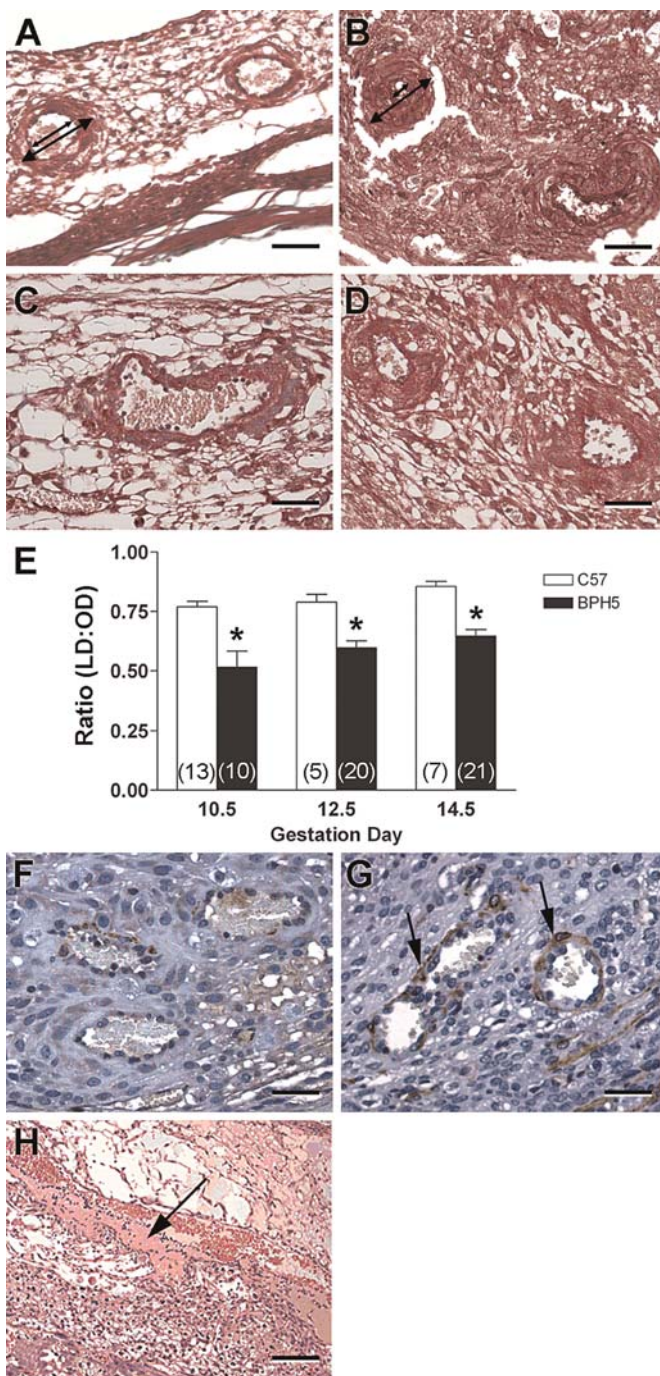


FIG. 4. Decidual vessels of BPH/5 placentas are characterized by narrowed lumens and thickened walls. **A**) Representative images of Masson Trichome-stained placental sections of C57 mice at E10.5 show the maternal vessels in the outer decidua with open lumens and thin arterial walls. **B**) In contrast, vessels in this region of the E10.5 BPH/5 placentas have narrowed lumens and a cuffed or onion-skin appearance, indicating a thickened arterial wall. **C** and **D**) These differences persist through mid-gestation, and are summarized as ratios of the inner lumen-to-outer diameter ratios (LD/OD) (**E**). Data are expressed as mean \pm SEM, and the numbers of vessels analyzed are shown on each summary bar. * $P < 0.05$ versus C57. Blood vessels in the corresponding serial decidual sections showed fewer actin-positive cells in C57 mice (**F**) compared to BPH/5 mice (**G**) ($n = 6-11$ placentas in each strain at E12.5, E14.5, and E18.5). Prominent PAS-stained fibrin-like fibrinoid deposits (arrow) are observed in BPH/5 placentas in the maternal decidua (**H**) throughout gestation. Fibrinoid deposits are rarely seen in C57 placentas (not shown). Bars = 50 μ m (**A-G**) and 200 μ m (**H**).

Altered Gene Expression Profiles in Placentas of BPH/5 Mice Starting Early in Gestation

To determine whether the architectural abnormalities observed in BPH/5 placentas are linked to quantitative changes in gene expression, real-time RT-PCR analyses were performed for several key trophoblast and/or angiogenesis-related transcripts in whole placental tissues from early, mid-, and late-gestation. As summarized in Figure 5, the mRNA levels of the prolactin/growth hormone family members and the trophoblast giant cell products of placental lactogens (chorionic somatomammotropin hormones) 1 and 2 (*Csh1* and *Csh2*) were dramatically reduced at E9.5 and E14.5. At E19.5, *Csh1* expression remained low compared to C57, whereas the *Csh2* levels had returned to the C57 levels by late gestation. Another member of this hormone family and a critical regulator of placental-specific angiogenesis, proliferin (*Plf*), showed strikingly reduced expression starting early in gestation, and these mRNA levels persisted throughout gestation. Interestingly, the proliferin antagonist proliferin-related protein (*Plfr*) was downregulated at early and mid-gestation but returned to the control level of expression by late gestation. Finally, consistent with our immunohistochemical data, the expression of the trophoblast invasion marker *Cdkn1c* was dramatically reduced at E9.5 and E14.5.

Compromised Maternal Placental Circulation in BPH/5 Mice

Given the vascular and developmental anomalies seen in BPH/5 placentas, we sought to determine whether this translated into compromised maternal-placental blood flow *in vivo* using pulse-wave Doppler analyses. Representative two-dimensional ultrasonograms of uterine arterial blood flow in BPH/5 and C57 mice at E16.5 revealed strikingly different profiles (Fig. 6, A and B). In BPH/5 mice, there was near-cessation of diastolic blood flow, which translated to a grossly elevated pulsatility index. An indicator of vascular resistance downstream of the Doppler-interrogated artery, this finding has been shown clinically to indicate placental vascular insufficiency [44]. From these data, we calculated and summarized the resistance indices, which further reflect significant impairment of the maternal-placental circulation in BPH/5 mothers compared to C57 controls (Fig. 6C).

DISCUSSION

While it has been strongly suggested that preeclampsia is caused by abnormal implantation and placental development, *i.e.*, events that occur during the early stages of pregnancy, research studies to date have mostly been limited to mid- to late-gestation after the maternal symptoms are manifest. As such, it has been difficult to determine the precise sequence of placental events, and to distinguish between primary causal mechanisms and secondary changes in the disease. Recently, we have identified an inbred mouse strain, BPH/5, which spontaneously develops the relevant clinical features of preeclampsia, including late-gestational hypertension, proteinuria, endothelial dysfunction, and fetal morbidity/mortality. In the present study, the goal was to characterize longitudinally the fetoplacental phenotype of this preeclampsia model in detail starting early in gestation. Our histological, immunohistochemical, morphometric, and gene expression analyses revealed that profound abnormalities in each of the placental zones are early hallmarks of the late-gestational maternal syndrome in BPH/5 mice. Furthermore, these early developmental and vascular anomalies translate into compromised uteroplacental circulation in these

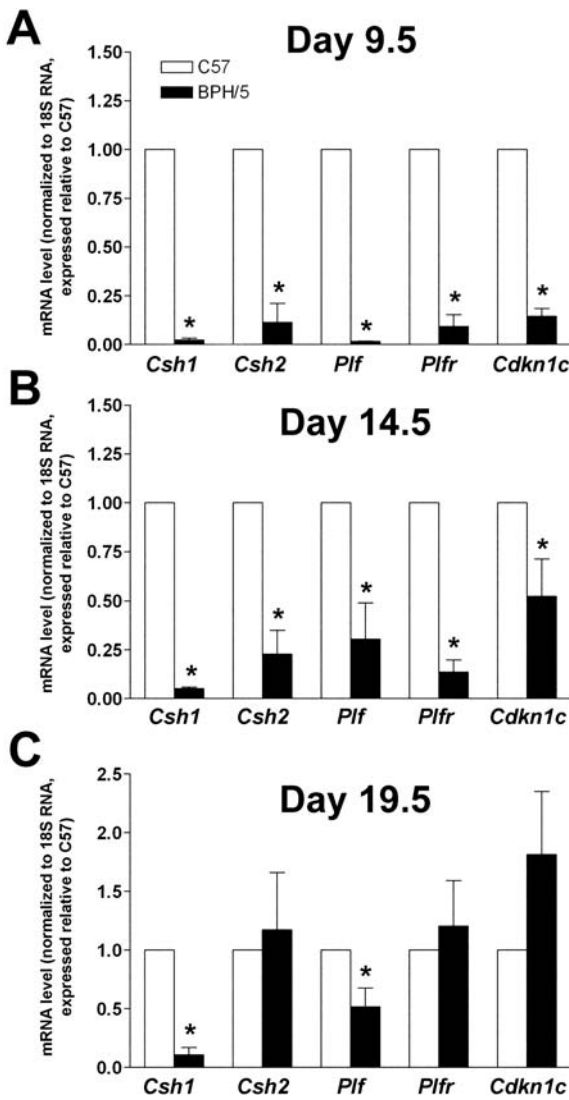


FIG. 5. BPH/5 placentas exhibit diminished expression of several key developmental factors starting early in gestation. Summary of quantitative real-time RT-PCR analyses of placental expression of *Csh1*, *Csh2*, *Plf*, *Plfr*, and *Cdkn1c* in C57 and BPH/5 mice at E9.5 (A), E14.5 (B) and E19.5 (C). Multiple placentas from each litter were pooled and the experiments were run in triplicate (n = 3–6 litters). * $P < 0.05$ versus timepoint-matched C57 controls.

mice. Together, these results support the hypothesis that defects at the maternal-fetal interface are primary causal events in preeclampsia, and further suggest that the BPH/5 model is an important tool for investigations of the underlying pathogenic mechanisms in this disease.

Our previous studies hinted at early pathological changes in the placenta of the BPH/5 mouse, with ultrasound and necropsy data demonstrating progressive intrauterine fetal demise starting prior to the spike in blood pressure and urinary protein levels [4]. In the present study, we have extended these findings and report significant reductions in BPH/5 fetal weights throughout pregnancy, with accompanying decreases in placental mass starting at E9.5. Although in general, the preeclamptic placenta is reported to be of normal weight and surface area at birth [45], our findings are consistent with the description of smaller placentas in women with severe preeclampsia and intrauterine growth restriction (IUGR) [46]. Interestingly, by late gestation, the difference in placental mass between BPH/5 and control mice was not significant, although

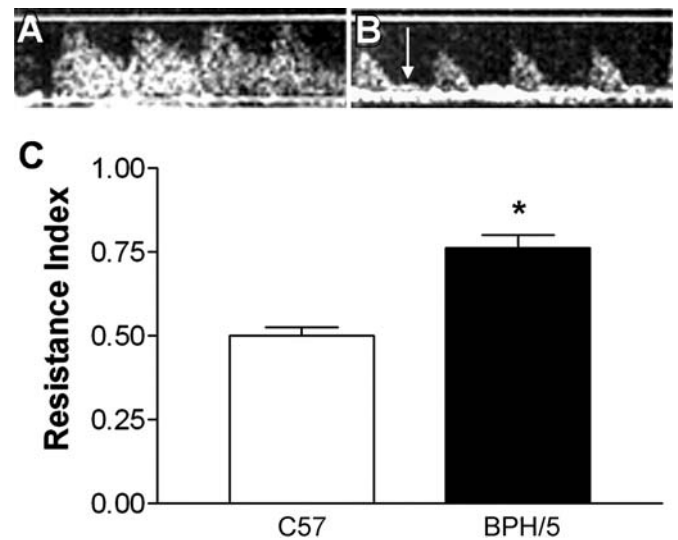


FIG. 6. Maternal-placental blood flow is compromised in BPH/5 mice. Representative pulse-wave Doppler profiles of uterine artery blood flow at E16.5 in C57 (A) and BPH/5 (B) mice. Near-cessation of blood flow during diastole (arrow) is seen in some BPH/5 mice. C) Summary of Doppler waveform analyses in C57 (n = 7) and BPH/5 (n = 6) mice at E16.5. Data are expressed as $1-[1/\text{pulsatility index}]$ to reflect resistance. * $P < 0.05$ versus C57.

it should be noted that fewer viable fetoplacental units remained at this gestational age. This may reflect a spectrum of placental pathology within litters, with only the healthiest subset of placentas supporting fetuses. However, it should be noted that even the surviving fetuses were smaller than their C57 counterparts.

Further detailed placental morphometric analyses revealed that, while all the placental cell lineages were present in BPH/5 mice, there were significant decreases in the proportional area occupied by the junctional zone. A complex layer that contains multiple cell types, including spongiotrophoblasts and glycogen cells, with a specialized subset of cells differentiating into trophoblast giant cells [47], the junctional zone is thought to play a pivotal role in decidual invasion, vascular remodeling, and other placental developmental processes [33, 48]. Using CDKN1C as a functional marker of trophoblast-mediated interstitial invasion [33], we detected very few CDKN1C-positive cells migrating into the maternal decidua of BPH/5 placentas compared to the control placentas. This was consistent with the gene expression data, which showed profound decreases in *Cdkn1c* transcript levels in BPH/5 placental samples from early- and mid-gestation. Given the recent evidence highlighting the importance of junctional zone trophoblasts and diffuse interstitial invasion in uterine vascular remodeling in murine placentas [49, 50], these data showing arrested trophoblast migration are consistent with our findings of impaired decidual arterial remodeling in BPH/5 mice. These data also support the results of studies in mice that are heterozygous for a *Cdkn1c* mutation, which exhibit trophoblast dysfunction and preeclampsia-like symptoms during pregnancy [11].

In these studies, the morphology and abundance of trophoblast giant cells at the periphery of the fetoplacental unit were not clearly altered in BPH/5 mice compared to C57 mice. Similarly, endo/perivascular invasion of central proximal decidual areas (indicated by cytokeratin staining), which is a process that is thought to be mediated by trophoblast giant cells [51], was not obviously different in BPH/5 mice. However, the mRNA levels of several factors produced by the giant cells, including *Csh1*, *Csh2*, *Cdkn1c*, and *Plf* [48], were profoundly

downregulated in BPH/5 mice starting early in gestation. The particularly robust and persistent downregulation of *Csh1* and *Plf* throughout pregnancy suggests a specific defect in endovascular giant cells, although decreased *Csh2* levels also suggests defects in the labyrinthine giant cells [52]. Given the important roles of these genes in placental development, vascularization, and function [48, 53], this suggests that trophoblast giant cell dysfunction has significant implications for this model. We focused initially on quantitative analysis of gene expression profiles using real-time RT-PCR but we recognize the importance of future *in situ* hybridization studies for spatiotemporal comparisons of these targets in BPH/5 and C57 placentas. Although the histological identification of trophoblast subtypes showed that all trophoblast populations were present, we cannot rule out the possibility that reductions in the expression levels of these genes were due to reductions in the numbers of specific cell types. Therefore, further studies aimed at the localization of these and other trophoblast markers in tissue sections will be important to quantify more precisely the various trophoblast populations in the BPH/5 placenta.

Maternal vascularization of the placenta to accommodate increased blood flow is one of the most important local adaptations to pregnancy, and dysregulation of this process is associated with preeclampsia [14, 15, 37]. Since abnormalities in the cell types and factors that mediate vascularization were detected early in BPH/5 pregnancy, we evaluated the uteroplacental circulation in these mice. In the normal mouse placenta, decidual arteries increase in diameter from E10.5–14.5. The radial arteries in the myometrial region have an intact endothelium and robust smooth muscle layer, whereas these arteries in the metrial triangle show an incomplete smooth muscle layer [42]. Further downstream into the decidua, no smooth muscle cells are detected surrounding the arteries, and eventually, endothelium-lined blood spaces are replaced by trophoblast-lined spaces in the junctional layer and labyrinth.

In the present study, we found that this vascular remodeling profile was dramatically altered in the BPH/5 strain compared to the C57 strain. Starting early in gestation, we observed that blood vessels traversing the decidua had significantly thickened arterial walls and narrowed lumens, translating into reduced lumen-to-outer diameter ratios. Furthermore, there was an abnormal persistence of smooth muscle cells in the walls of these vessels. This suggests that the critical transformation of these vessels into large flaccid conduits to accommodate increased blood flow to the fetus is abnormal in BPH/5 mice. Early downregulation of genes that encode the murine placenta-specific angiogenic factor *Plf*, along with its regulator *Plfr*, further support the notion that vascularization is abnormal in BPH/5 mice. *Plf* stimulates endothelial cell migration and neovascularization and plays a role in the reorganization and growth of maternal uterine blood vessels towards the developing fetus [53]. Indeed, the majority of the soluble angiogenic activity secreted by the midgestation placenta, as measured by an endothelial cell chemotaxis assay, is attributable to *Plf* [53].

Inadequate remodeling of the uterine arteries is correlated with the development of abnormal uterine artery blood flow in women [44, 54]. Evidence suggests that increased uterine artery resistance documented in the second trimester indicates placental insufficiency and is predictive of high-risk human pregnancies, including those associated with intrauterine growth restriction and preeclampsia [44]. Iatrogenic reductions in uterine blood flow in a number of animal models have also been shown to induce a hypertensive state that resembles preeclampsia [7, 55]. In our study, ultrasound investigation of uterine arteries revealed significant alterations in the Doppler profiles of BPH/5 mice at E16.5, which indicates marked

decreases in downstream blood flow, i.e., placental vascular resistance. This suggests that the decidual vascular pathology observed in this model is associated with reduced fetoplacental perfusion. Given our evidence of vessel abnormalities as early as E10.5, we speculate that these early defects lead to reduced uteroplacental blood flow. However, the limitations of this technology in terms of obtaining reliable Doppler flow profiles of the uterine artery earlier than E16.5 prevented us from establishing definitively the exact time-course relative to abnormal placentation. Nonetheless, these findings are important with regard to establishing functional placental insufficiency, and provide a possible explanation for the fetal growth restriction/demise in this model.

Preeclampsia in women is also strongly associated with defects in development and vascularization in the fetal compartment [56]. In addition to maternal vascular remodeling defects in BPH/5 mice, the fetal labyrinth showed impaired branching morphogenesis and reduced expansion toward the junctional zone. Together with anomalous organization of the labyrinthine trophoblast layers, this probably results in a decreased surface area for nutrient and gas exchange in this model [57]. Given the important role of trophoblast function in labyrinthine development [26], it is important to note that these architectural changes in the fetal compartment coincided with several indices of trophoblast impairment in our study, e.g., reduced *Cdkn1c* expression and decreased junctional zone thickness.

In summary, the BPH/5 mouse model displays the cardinal features of human preeclampsia, and our results show that severe abnormalities in placentation precede the development of the syndrome in these mice. However, the relative roles of maternal susceptibility and fetoplacental factors in causing preeclampsia in this model remain under investigation. Since the BPH/5 strain exhibits mildly elevated blood pressure even before pregnancy, it is possible that impaired placentation is the result of predisposition to hypertension. An alternative possibility is that the borderline hypertension and placental pathology are independent defects that interact to produce preeclampsia in this model. To test these hypotheses directly, we are currently performing reciprocal embryo transfer experiments, whereby BPH/5 females are made pregnant by transfer of wild-type embryos and vice versa. Since abnormal placental development is hypothesized to be the central event leading to preeclampsia, we believe this model will be helpful in clarifying the sequence of changes and dissecting the underlying molecular mechanisms of this syndrome. In addition, BPH/5 mice should provide a useful model system for determining the underlying genetic defects, identifying diagnostic strategies, and testing therapeutic approaches.

ACKNOWLEDGMENTS

We acknowledge the expert assistance of Paul Reimann and Dennis Dunwald in generating the figures.

REFERENCES

1. Martin JA, Hamilton BE, Sutton PD, Ventura SJ, Menacker F, Munson ML. Births: final data for 2003. Natl Vital Stat Rep 2005; 54:1–116.
2. MacKay AP, Berg CJ, Atrash HK. Pregnancy-related mortality from preeclampsia and eclampsia. Obstet Gynecol 2001; 97:533–538.
3. Duley L. Maternal mortality associated with hypertensive disorders of pregnancy in Africa, Asia, Latin America and the Caribbean. Br J Obstet Gynaecol 1992; 99:547–553.
4. Davison RL, Hoffmann DS, Butz GM, Aldape G, Schlager G, Merrill DC, Sethi S, Weiss RM, Bates JN. Discovery of a spontaneous genetic mouse model of preeclampsia. Hypertension 2002; 39:337–342.
5. Sibai BM, Abdella TN, Anderson GD. Pregnancy outcome in 211 patients with mild chronic hypertension. Obstet Gynecol 1983; 61:571–576.

6. Sibai BM, Ewell M, Levine RJ, Klebanoff MA, Esterlitz J, Catalano PM, Goldenberg RL, Joffe G. Risk factors associated with preeclampsia in healthy nulliparous women. The Calcium for Preeclampsia Prevention (CPEP) Study Group. *Am J Obstet Gynecol* 1997; 177:1003–1010.
7. Alexander BT, Kassab SE, Miller MT, Abram SR, Reckelhoff JF, Bennett WA, Granger JP. Reduced uterine perfusion pressure during pregnancy in the rat is associated with increases in arterial pressure and changes in renal nitric oxide. *Hypertension* 2000; 37:1191–1195.
8. Alexander BT, Cockrell KL, Massey MB, Bennett WA, Granger JP. Tumor necrosis factor-alpha-induced hypertension in pregnant rats results in decreased renal neuronal nitric oxide synthase expression. *Am J Hypertens* 2002; 15:170–175.
9. Yallampalli C, Garfield RE. Inhibition of nitric oxide synthesis in rats during pregnancy produces signs similar to those of preeclampsia. *Am J Obstet Gynecol* 1993; 169:1316–1320.
10. Maynard SE, Min JY, Merchan J, Lim KH, Li J, Mondal S, Libermann TA, Morgan JP, Sellke FW, Stillman IE, Epstein FH, Sukhatme VP, et al. Excess placental soluble fms-like tyrosine kinase 1 (sFlt1) may contribute to endothelial dysfunction, hypertension, and proteinuria in preeclampsia. *J Clin Invest* 2003; 111:649–658.
11. Kanayama N, Takahashi K, Matsuura T, Sugimura M, Kobayashi T, Moniwa N, Tomita M, Nakayama K. Deficiency in p57Kip2 expression induces preeclampsia-like symptoms in mice. *Mol Hum Reprod* 2002; 8: 1129–1135.
12. Chun D, Braga C, Chow C, Lok L. Clinical observations on some aspects of hydatidiform moles. *J Obstet Gynaecol Br Commonw* 1964; 71:180–184.
13. Goldstein DP, Berkowitz RS. Current management of complete and partial molar pregnancy. *J Reprod Med* 1994; 39:139–146.
14. Brosens IA, Robertson WB, Dixon HG. The role of the spiral arteries in the pathogenesis of preeclampsia. *Obstet Gynecol Annu* 1972; 1:177–191.
15. Kaufmann P, Black S, Huppertz B. Endovascular trophoblast invasion: implications for the pathogenesis of intrauterine growth retardation and preeclampsia. *Biol Reprod* 2003; 69:1–7.
16. Redman CW, Sargent IL. Latest advances in understanding preeclampsia. *Science* 2005; 308:1592–1594.
17. Hirano H, Imai Y, Ito H. Spiral artery of placenta: development and pathology-immunohistochemical, microscopical, and electron-microscopic study. *Kobe J Med Sci* 2002; 48:13–23.
18. Zhou Y, Damsky CH, Fisher SJ. Preeclampsia is associated with failure of human cytotrophoblasts to mimic a vascular adhesion phenotype. One cause of defective endovascular invasion in this syndrome? *J Clin Invest* 1997; 99:2152–2164.
19. Caniggia I, Grisar-Gravnosky S, Kuliszewsky M, Post M, Lye SJ. Inhibition of TGF-beta 3 restores the invasive capability of extravillous trophoblasts in preeclamptic pregnancies. *J Clin Invest* 1999; 103:1641–1650.
20. Redline RW, Patterson P. Pre-eclampsia is associated with an excess of proliferative immature intermediate trophoblast. *Hum Pathol* 1995; 26: 594–600.
21. Zhou Y, McMaster M, Woo K, Janatpour M, Perry J, Karpanen T, Alitalo K, Damsky C, Fisher SJ. Vascular endothelial growth factor ligands and receptors that regulate human cytotrophoblast survival are dysregulated in severe preeclampsia and hemolysis, elevated liver enzymes, and low platelets syndrome. *Am J Pathol* 2002; 160:1405–1423.
22. Roberts JM, Lain KY. Recent insights into the pathogenesis of preeclampsia. *Placenta* 2002; 23:359–372.
23. Rasmussen S, Irgens LM. Fetal growth and body proportion in preeclampsia. *Obstet Gynecol* 2003; 101:575–583.
24. Long PA, Abell DA, Beischer NA. Fetal growth retardation and preeclampsia. *Br J Obstet Gynaecol* 1980; 87:13–18.
25. Rossant J, Cross JC. Placental development: lessons from mouse mutants. *Nat Rev Genet* 2001; 2:538–548.
26. Cross JC, Baczyk D, Dobric N, Hemberger M, Hughes M, Simmons DG, Yamamoto H, Kingdom JC. Genes, development and evolution of the placenta. *Placenta* 2003; 24:123–130.
27. Georgiades P, Ferguson-Smith AC, Burton GJ. Comparative developmental anatomy of the murine and human definitive placentae. *Placenta* 2002; 23:3–19.
28. Schlager G, Lester JW, Carrithers JA. Characteristics of the inbred hypertensive mouse strains. *FASEB J* 1989; 3:A1315.
29. Schlager G. Biometrical genetic analysis of blood pressure level in the genetically hypertensive mouse. *Clin Exp Hypertens* 1994; 16:809–824.
30. Schlager G. Genetic hypertension in mice. In: Ganten D, DeJong W, (eds.), *Handbook of Hypertension*. Amsterdam: Elsevier; 1994:158–172.
31. Lester JW. Survey of selected physiological properties of inbred hypertensive and hypotensive mice. Kansas, USA: University of Kansas; 1989. Thesis.
32. Laitinen L. Griffonia simplicifolia lectins bind specifically to endothelial cells and some epithelial cells in mouse tissues. *Histochem J* 1987; 19: 225–234.
33. Takahashi K, Kobayashi T, Kanayama N. p57(Kip2) regulates the proper development of labyrinthine and spongiotrophoblasts. *Mol Hum Reprod* 2000; 6:1019–1025.
34. Vercauysse L, Caluwaerts S, Luyten C, Pijnenborg R. Interstitial trophoblast invasion in the decidua and mesometrial triangle during the last third of pregnancy in the rat. *Placenta* 2006; 27:22–33.
35. Croy BA, Ashkar AA, Minhas K, Greenwood JD. Can murine uterine natural killer cells give insights into the pathogenesis of preeclampsia? *J Soc Gynecol Invest* 2000; 7:12–20.
36. Georgiades P, Watkins M, Burton GJ, Ferguson-Smith AC. Roles for genomic imprinting and the zygotic genome in placental development. *Proc Natl Acad Sci U S A* 2001; 98:4522–4527.
37. Pijnenborg R, Robertson WB, Brosens I, Dixon G. Review article: trophoblast invasion and the establishment of haemochorial placentation in man and laboratory animals. *Placenta* 1981; 2:71–91.
38. Muntener M, Hsu YC. Development of trophoblast and placenta of the mouse. A reinvestigation with regard to the in vitro culture of mouse trophoblast and placenta. *Acta Anat (Basel)* 1977; 98:241–252.
39. Hemberger M, Cross JC, Ropers HH, Lehrach H, Fundele R, Himmelbauer H. UniGene cDNA array-based monitoring of transcriptome changes during mouse placental development. *Proc Natl Acad Sci U S A* 2001; 98:13126–13131.
40. Hill JA, Karimi M, Kutschke W, Davisson RL, Zimmerman K, Wang Z, Kerber RE, Weiss RM. Cardiac hypertrophy is not a required compensatory response to short-term pressure overload. *Circulation* 2000; 101:2863–2869.
41. Chaoui R, Hoffmann H, Bollmann R, Halle H, Zienert A, Metzner A. [Assessment of uteroplacental circulation in uncomplicated pregnancies using pulsed Doppler ultrasound]. *Zentralbl Gynakol* 1990; 112:11–18.
42. Adamson SL, Lu Y, Whiteley KJ, Holmyard D, Hemberger M, Pfarrer C, Cross JC. Interactions between trophoblast cells and the maternal and fetal circulation in the mouse placenta. *Dev Biol* 2002; 250:358–373.
43. Mayhew TM. Thinning of the intervacular tissue layers of the human placenta is an adaptive response to passive diffusion in vivo and may help to predict the origins of fetal hypoxia. *Eur J Obstet Gynecol Reprod Biol* 1998; 81:101–109.
44. Parra M, Rodrigo R, Barja P, Bosco C, Fernandez V, Munoz H, Soto-Chacon E. Screening test for preeclampsia through assessment of uteroplacental blood flow and biochemical markers of oxidative stress and endothelial dysfunction. *Am J Obstet Gynecol* 2005; 193:1486–1491.
45. Teasdale F. Histomorphometry of the human placenta in maternal preeclampsia. *Am J Obstet Gynecol* 1985; 152:25–31.
46. McMaster MT, Zhou Y, Fisher SJ. Abnormal placentation and the syndrome of preeclampsia. *Semin Nephrol* 2004; 24:540–547.
47. Carney EW, Pridaux V, Lye SJ, Rossant J. Progressive expression of trophoblast-specific genes during formation of mouse trophoblast giant cells in vitro. *Mol Reprod Dev* 1993; 34:357–368.
48. Linzer DI, Fisher SJ. The placenta and the prolactin family of hormones: regulation of the physiology of pregnancy. *Mol Endocrinol* 1999; 13:837–840.
49. Pijnenborg R, Vercauysse L, Hanssens M. The uterine spiral arteries in human pregnancy: facts and controversies. *Placenta* 2006; 27:939–958.
50. Carter AM, Enders AC, Jones CJ, Mess A, Pfarrer C, Pijnenborg R, Soma H. Comparative Placentation and animal models: patterns of trophoblast invasion - a workshop report. *Placenta* 2006; 27 Suppl A:530–533.
51. Cross JC. How to make a placenta: mechanisms of trophoblast cell differentiation in mice - a review. *Placenta* 2005; 26(suppl A):S3–S9.
52. Simmons DG, Cross JC. Determinants of trophoblast lineage and cell subtype specification in the mouse placenta. *Dev Biol* 2005; 284:12–24.
53. Jackson D, Volpert OV, Bouck N, Linzer DI. Stimulation and inhibition of angiogenesis by placental proliferin and proliferin-related protein. *Science* 1994; 266:1581–1584.
54. Iwata M, Matsuzaki N, Shimizu I, Mitsuda N, Nakayama M, Suehara N. Prenatal detection of ischemic changes in the placenta of the growth-retarded fetus by Doppler flow velocimetry of the maternal uterine artery. *Obstet Gynecol* 1993; 82:494–499.
55. Abitbol MM, Gallo GR, Pirani CL, Ober WB. Production of experimental toxemia in the pregnant rabbit. *Am J Obstet Gynecol* 1976; 124:460–470.
56. Mayhew TM, Charnock-Jones DS, Kaufmann P. Aspects of human fetoplacental vasculogenesis and angiogenesis. III. Changes in complicated pregnancies. *Placenta* 2004; 25:127–139.
57. Cross JC, Simmons DG, Watson ED. Chorioallantoic morphogenesis and formation of the placental villous tree. *Ann N Y Acad Sci* 2003; 995:84–93.